DRAFT (2)
Aug 92

1992

Field Observations of Infragravity, Sea and Swell Directional Spectra

by

Joan Oltman-Shay

QUEST Integrated, Inc., 21414 68th Ave. So.

Kent, WA. 98032

Abstract

Infragravity, sea and swell wavenumber-frequency (k-f) spectra from an alongshore-aligned array of bottom-mounted pressure sensors in 8 m depth (800 m offshore) are analyzed for their insight into edge wave generation mechanisms. Eight months of nearly continuous data are analyzed. Earlier analysis of infragravity k-f spectra from this site identified the presence of trapped edge waves, distinct from leaky waves at this offshore location (Oltman-Shay et al., 1992). Here, edge wave variance is separated from other infragravity motions (leaky and bound waves) by their k-f location in the spectra. It is observed that on average edge waves account for ~50% of the total infragravity variance at this offshore location, and occasionally dominate with ~80% of the variance. Significant wave heights greater than 20 cm are observed. Correlation analysis of up- and downcoast progressive edge wave variance with sea and swell directional distributions suggest that swell waves propagating from the same directional quadrant as the edge wave are the dominant generation source; sea waves had significantly lower correlations. An order of magnitude difference in of up- and downcoast progressive edge wave variance is occasionally observed and is shown to be expected from the theory of resonant excitation of edge waves through nonlinear difference interaction of swell waves incident to the beach at oblique angles to the normal. The correlation between swell and edge waves from the same directional quadrant is approximately linear and accounts for more than 90% of the up- and downcoast edge wave variance over the 8 months.

St-A per telecon, Dr. Jacobson, ONR/ Code 3242. Arl., VA 22217.
7-9-93 JK

Introduction

Infragravity waves (nominally 0.005-0.05 Hz) are an important process in the nearshore. Initially, these surface gravity waves received attention because of the recognition that their length scales ($O(10^2\text{-}10^3$ m) are similar to those of common nearshore morphological features such as linear and crescentic sand bars (Bowen and Inman, 1971; Lau and Travis, 1973; Short, 1975; Bowen, 1980; Holman and Bowen, 1982) and later because of the observation that infragravity band energy can dominate sea and swell (nominally 0.05-0.35 Hz) energy in the surf zone (Guza and Thornton, 1982; Holman and Bowen, 1984). It is widely accepted that infragravity waves derive their momentum from sea and swell; the magnitude of their phase velocity precluding them from generation directly by the wind. The hypothesized models of generation are described in terms of nonlinear triad interactions (Gallagher, 1971; Bowen and Guza, 1978) or radiation stresses gradients (Longuet-Higgins and Stewart, 1962, 1964; Symonds et al., 1982; Scaffer and Svendson, 1988; Schaffer, 1990) of sea and swell. Research over the past two decades has been directed at understanding the wave mode content of this frequency band, the generation mechanisms, dissipation, and the interplay of these waves with a movable sandy bed.

Theory and field observation identify three kinematically distinct infragravity waves. Infragravity bound waves have a wavenumber-frequency distribution that does not satisfy the linear dispersion equation for free surface gravity waves and must therefore travel with the waves that force them. Infragravity edge and leaky waves satisfy the linear dispersion relation and can propagate away from the generation source. Edge waves are refractively trapped towards the shoreline of a sloping beach and have a set of modes (n = 0,1,2,3...) which satisfy the boundary conditions of the nearshore waveguide. Leaky waves are more normally incident to the beach and can escape out to deep water upon reflection at the shoreline.

Distinguishing edge and leaky infragravity waves in field observations has proven difficult. However, the utilization of coherent alongshore arrays of sensors from which alongshore wavenumber-frequency (k-f) spectra of infragravity energy can be estimated has been useful in identifying low mode (< 3) edge waves (Huntley et al, 1981; Oltman-Shay and Guza, 1987; and Howd et. al, 1991). In these surf zone observations of infragravity k-f variance, low mode edge waves were observed to dominate the alongshore component of velocity with as much as 88% of the variance. The cross-shore component of velocity appeared to be dominated by either high mode edge waves and/or leaky waves; identifying one from the other was not possible because their alongshore wavenumbers were unresolved. However, more recently, Oltman-Shay et al. (1992) have analyzed array data 800 m offshore and identified edge waves, resolvable from leaky waves, by their k-f spectral location and cross-shore variance structure.

Here, infragravity, sea and swell wavenumber-frequency (k-f) spectra from an alongshore-aligned array of bottom-mounted pressure sensors in 8 m depth (800 m offshore) are analyzed for their insight into edge wave generation mechanisms. Eight months of nearly continuous data are analyzed. Edge wave variance is separated from other infragravity motions (leaky and bound waves) by their k-f location in the spectra. In section 2, the field site, data acquisition and processing are described followed by a presentation variance and correlation analysis (section 3). The observations are discussed and summarized in section 4.

Field Site and Analysis Methods

Field measurements of infragravity, sea and swell directional spectra were made during the SAMSON (Sept. 90-May91) and DELILAH (Oct 90) experiments off the coast of the Coastal Engineering Research Center's Field Research Facility (FRF) in Duck, North Carolina. Duck is located in the middle of a 100 km-long barrier spit known as the Outer Banks of North Carolina. It is a straight, east-facing, and sandy beach. The closest interruption is a 500 m long cement pier ~500 m to the south of the main instrument line. Deep troughs about the pier and the presence of an alongshore-aligned, submerged sand bar ~60 m offshore, that moves from linear (equal distance offshore) to crescentic (modulated distance offshore), break the otherwise shore-parallel bathymetry (Figure 1).

An alongshore-aligned array of bottom-mounted pressure sensors 800 m offshore has been maintained by the FRF at this site since Fall 1986. The array was designed to measure the incident sea and swell directional field. The original design comprised nine sensors placed equal distance offshore along the 8 m depth contour. The array spans 255 m alongshore with a minimum sensor separation of 5 m. In the summer of 1990, 5 additional pressure sensors were placed in a cross-shore line through the linear array, spanning 120 m. Data were acquired from this array for the SAMSON experiment at 4 Hz in 170 minute length blocks every 3 hours, with the 10 minute gaps for data transfer to storage media. After December 1 1990, data continued to be collected for SAMSON scientists through 1 June 1991, but was reduced to 170 minute blocks every 6 hours. Only the alongshore-aligned component of the array will be analyzed for this paper.

During the DELILAH experiment, cross-shore bathymetric transects measuring depth at ~1-3 m cross-shore intervals out to ~400 m were acquired daily using the FRF's Coastal Research Amphibious Buggy (CRAB; Birkemeier and Mason, 1984); these measurements are part of the FRF's long term monitoring system and are otherwise acquired on a monthly schedule, more frequently with storm events. There were 20

transects, spaced every 25 m within the DELILAH instruments, and 50 m outside. The total alongshore coverage was 500 m. Several surveys out to 13 m depth (~ 2 km offshore) were also acquired.

Wavenumber spectra were estimated from these arrays using the Iterative Maximum Likelihood Estimator (IMLE; Pawka, 1982, 1983). The IMLE is a high resolution estimator well-suited for estimation of signals in noise. This estimator has been used in previous analyses of infragravity wavenumber variance (Oltman-Shay and Guza, 1987; Oltman-Shay et al., 1989; Howd et al., 1991; Oltman-Shay et al., 1992) and sea and swell variance (Pawka, 1982; Long and Oltman-Shay, 1991).

Observations

The correlation between infragravity waves and incident sea and swell waves has been noted since infragravity waves were first observed in the field. Munk (1949) and Tucker (1950) noted significant correlations between the fluctuation of incident wave heights (groupiness) and the infragravity motions. Infragravity variance has been repeatedly been shown to increase with incident wave (Guza and Thornton, 1982; Sallenger and Holman, 1984; Holman and Sallenger, 1985). Figure 2 examples infragravity and sea and swell significant wave height for one month of this 8 month data set. The infragravity wave heights ranges from 5 to 25 cm over the 8 months, sea and swell range 10 to 400 cm and 10 to 600 cm, respectively. The 8 months of data also provide a variety sea and swell directional distributions.

In the following we continue the investigation of the causative correlation between sea, swell and infragravity waves with a breakdown of infragravity variance into the kinematically distinctive trapped and leaky waves.

Wavenumber Partitioning of Infragravity Variance

In this section, alongshore wavenumber-frequency (k-f) spectra are used to partition infragravity variance between trapped and leaky wave modes. Figure 3 shows two example spectra. The wavenumber Nyquist of the array is 0.1 m^{-1}, however insignificant variance is contained outside the maximum displayed wavenumber (0.01 m^{-1}). For reference, deep water, local depth, and mode 0 (edge wave) surface gravity wave dispersion curves are drawn. The curves are shown for both up- and downcoast propagating waves, mirrored about zero alongshore wavenumber.

There are two domains in k-f space that will be generically referenced as the leaky and trapped domains. These domains are identified for both their kinematic and dynamic differences. The leaky domain is that

wavenumber space centered on zero alongshore wavenumber, bounded by the deep water dispersion curves. The trapped domain occupies the space between the deep water dispersion curve and the lowest (0) edge wave mode. Both leaky and bound waves can occupy any region in the leaky domain continuum. The trapped domain can contain shallow-water generated edge or bound waves. The edge waves lie on the set of dispersion curves; the bound waves can occupy any region in this domain.

The spectra in Figure 3 show variance peaks both in the trapped and leaky domains. The variance in the trapped domain falling along the local dispersion curve has been shown to be edge waves, as opposed to bound waves (Oltman-Shay et al., 1992). In Figure 3a, near equal amounts of north- and southward propagating edge waves are indicated in the spectrum, with a near-equivalent amount of leaky wave variance. Swell waves also fall within this leaky wave domain, identified by the increase in variance at frequencies above 0.056 Hz. In contrast, Figure 3b shows unequal amounts of north- and southward propagating edge waves and relatively less leaky wave variance.

In the following, three variance quantities will be discussed: the trapped, leaky and edge wave variance. The trapped variance is summed across wavenumber space between the mode 0 and the deep water dispersion curve for both north- and southward propagating waves. The leaky variance is summed between the deep water dispersion curves, through the zero alongshore wavenumber (normal incidence). The spectral leakage of leaky wave variance into the trapped domain (e.g. Figure 3a) was recognized and accommodated by slightly adjusting the limits of integration (Figure 4).

The trapped variance is further partitioned to investigate the variance that has been shown to be edge waves, as opposed to bound waves (Oltman-Shay et al., 1992), by summing across the variance ridge that lies along the local dispersion curve. The f-k location of this ridge does not change over the 8 months, thus the variance is summed between the local dispersion curve and the local dispersion curve - epsilon, where epsilon is fixed and chosen so that the integration typically spans the full half-power bandwidth of the spectral peaks (Figure 4). An upper frequency limit of 0.04 Hz for all variance quantities was chosen to avoid swell variance. A lower limit of 0.02 Hz was necessary because the edge wave variance peaks are not resolvable from the leaky domain below this frequency.

The ratios of trapped, leaky and total edge wave (north- and southward propagation) to total infragravity variance, in the 0.02 to 0.04 Hz band, are shown in Figure 5 for the 8 months analyzed. Variance in the trapped domain (which recall contains both edge and bound waves) is typically higher than in the leaky wave domain at this site (Figures 5a,b). The edge waves identified in the trapped domain on average make

up approximately 50% of the total infragravity variance (Figure 5c). However as much as 80% of the infragravity can be at times attributed to edge waves.

Infragravity, Sea and Swell Variance

Infragravity variance was shown by Elgar et al. (1992) to have a higher correlation with swell than sea variance at this site and several others. This is again shown for the smaller infragravity frequency band (0.02 - 0.04 Hz) used here (Figure 6a). Utilizing the k-f partitioned variance, the trapped, leaky and total edge wave variances are also compared against sea and swell (Figures 6b,c,d). Variance in all of the domains show a statistically significant higher correlation with swell than sea with differences in regression slopes as well (Table 1a).

Edge, sea and swell wave variances are further partitioned by the direction of propagation. In figure 7, edge wave variance propagating northward (southward) is plotted against sea and swell wave variance propagating from the north (south) quadrant. Again, the low correlation of edge and sea wave variance is observed. However, edge and swell waves propagating from the same directional quadrant are highly correlated (Table 1b). In contrast, edge and swell waves propagating from opposite quadrants are not as well correlated (Figure 8, Table 1b).

Discussion and Summary

Wavenumber-frequency (k-f) spectra of infragravity surface elevation variance 800 m offshore of Duck, North Carolina are analyzed for wave mode content in a study spanning eight months of nearly continuous data. Wave variance trapped in the nearshore (as opposed to variance that can escape the nearshore) on average dominates the infragravity band with ~70% of the total variance (Figure 5). Variance identified as edge waves accounts for ~50% of the total variance, and occasionally dominates with ~80% of the variance (Figure 5). Significant wave heights greater than 20 cm are observed. It is important to note that 20 cm significant wave heights of infragravity edge waves 800 m offshore of this beach imply shoreline wave heights of (very) roughly 75 cm, where the exponential decay, exp(-kx) for an edge wave is applied to the offshore variance with a nominal k of 0.003 m-1(the average wavenumber in the frequency band). However, this extreme shoreline wave height estimate is a lower limit because the variance of lower modes trapped shoreward of the 800m location is not included and the edge wave frequency band for this wave height estimate is a subset of the infragravity edge wave frequencies.

Correlation analysis of up- and downcoast progressive edge wave variance with sea and swell directional distributions suggest that swell waves propagating from the same directional quadrant as the edge wave are the dominant generation source; sea waves had significantly lower correlations, as did swell waves propagating from directional quadrants different from the edge waves (Figures 6, 7 and 8, Table 1). The association of swell and edge wave from the same directional quadrant is also observed by the order of magnitude difference in the amount of up- and downcoast progressive edge wave variance at this field site when there is strong swell incident at oblique angles to the beach normal (e.g. Figure 3b). The correlation between swell and edge waves from the same directional quadrant is approximately linear and accounts for more than 90% of the up- and downcoast edge wave variance over the 8 months.

A question that immediately arises is whether present edge wave generation theory can account for both the high correlation between edge waves and swell waves (as opposed to sea waves), and the higher correlation of swell and edge waves from the same directional quadrant (as opposed to different directional quadrants). The answer to the swell wave correlation is no. The only spectral edge wave generation model is from Gallagher (1971), where the nonlinear triad interaction of two incident waves with an edge wave is described through a coupling coefficient. However, the behavior of these coupling coefficients has not been studied, the biggest reason being the breakdown of the model in the surf zone where much of the edge wave resonant forcing is likely occurring. On the other hand, it is noteworthy that bound wave theory, which does not have this problem, indicates that the coupling coefficients between interacting incident waves and the bound wave in shallow water are larger for swell wave forcing than for sea wave forcing (Sand, 1982, Okihiro et al, 1992).

However, a reason for the high correlation between swell and edge waves propagating from the same directional quadrant can be found in the Gallagher (1971) triad interaction description of edge wave forcing. Fundamental to these triad interactions is that the difference interaction of the two incident waves must satisfy the dispersion relation of the edge wave mode. Bowen and Guza (1978) examined incident wave frequency and directional conditions for resonant excitation of edge wave modes and propagation directions. In Figure 9, their approach is used to compare resonance conditions for a 0.003 Hz edge waves excited by swell-swell wave interactions (centered about 0.07 Hz) and sea-sea wave interactions (centered about 0.02 Hz). The cross-hatched area represents the mix of the sea (Figure 9b) and swell (Figure 9a) incident wave directional combinations obtained from a simulated directional distribution with a peak direction 15 degrees from the normal to the beach, α_1 is the direction of propagation of the 0.070 (0.020) Hz incident wave and α_2 is the propagation direction of the 0.070 minus 0.003 (0.020 minus 0.003) Hz incident wave. The solid

lines marked 0, 1, 2, etc. are for each edge wave mode and indicate which directional pairs of incident waves can resonantly excite these waves. The +k and -k indicate edge wave propagation up- and down-coast and the region lying between the +k and -k highest mode edge waves is the region of leaky wave excitation. Figure 9a indicates that for this simulated incident directional distribution of off normal incidence, nonlinear resonant difference interactions between swell waves will excite only edge waves propagating from the same directional quadrant. However, Figure 9b shows that nonlinear difference interaction of sea waves will not yield preferential edge wave propagation directions. Thus there is a somewhat circular agreement between observation and the triad interaction mechanism where sea-sea interactions cannot explain the observed preferential excitation of edge waves propagation direction, but swell-swell interactions can, and observations indicate that swell waves are more highly correlated with edge waves.

Acknowledgments

Field data collection and analysis support was provided by the Office of Naval Research, Coastal Sciences (contract N00014-90-1118) and Geology and Geophysics (contract N00014-91-C-0004). The U.S. Army Corps of Engineers Field Research Facility (FRF) hosted the experiment and the Field Research Facility Infragravity Waves in the Nearshore Zone work unit of the Coastal Flooding and Storm Protection Program, Coastal Engineering and Research and Development program, U.S. Army Corps of Engineers provided additional analysis support. The skill and determination of the personnel at the FRF, under the directorship of Bill Birkemeier, saw this large and ambitious field effort through to success. Ed Thornton and Bob Guza's seasoned field crews also contributed greatly to instrument deployment and acquisition. Chuck Long, Kent Hathaway and Steve Elgar were invaluable compatriots in the acquisition of this data set.

DACW39-91-C-0021

References

Birkemeier, W.A. and Mason,C., 1984, "The Crab: A unique nearshore surveying vehicle," ASCE *J. Surv. Eng.*, vol. 110, no. 1, pp. 1-7.

Bowen, A.J. and D.L. Inman, 1971, "Edge waves and crescentic bars," *J. Geophys. Res.*, **76**, 8662-8671.

Bowen, A.J. and R.T. Guza, 1978, "Edge waves and surf beat," *J. Geophys. Res.*, **83**, 1913-1920.

Bowen, A.J., 1980, "Simple models of nearshore sedimentation: beach profiles and longshore bars, " In: S.B. McCann (Editor), Coastline of Canada, Littoral Processes and Shore Morphology, Geol. Surv. Can., Pap., 80-10, 1-11.

Elgar, S. T.H.C. Herbers, M. Okihiro, J. Oltman-Shay and R.T. Guza, 1992 (*in press*), "Observations of Infragravity Waves," *J. Geophys. Res.*

Gallagher, B., 1971, "Generation of surf beat by non-linear wave interaction", *J. Fluid Mech.*, **49**(1), 1-20.

Guza, R.T. and E.B. Thornton, 1982, "Swash oscillations on a natural beach," *J. Geophys. Res.*, **87**, 483-491.

Holman, R.A., 1981, "Infragravity energy in the surf zone," *J. Geophys. Res.*, **86**, 6442-6450.

Holman, R.A. and A.J. Bowen, 1982, "Bars, bumps and holes: models for the generation of complex beach topography, " *J. Geophys. Res.*, **87**, 457-468.

Holman, R.A. and A.J. Bowen, 1984, "Longshore structure of infragravity wave motions, " *J. Geophys. Res.*, **89**, 6446-6452.

Holman, R.A. and A.H. Sallenger, 1985, "Setup and swash on a natural beach," *Journ. of Geophy. Res.*, **90**(C1) 945-953.

Howd, P.A., J. Oltman-Shay and R.A. Holman, 1991, "Wave variance partitioning in the trough of a barred beach," *J. Geophys. Res.*, **96**, 12,781-12,795.

Huntley, D.A., R.T. Guza and E.B. Thornton, 1981, "Field observations of surf beat, 1. Progressive edge waves," *J. Geophys. Res.*, **86**, 6451-6466.

Lau, J. and B. Travis, 1973, "Slowly varying Stokes waves and submarine longshore bars," *J. Geophys. Res.*, **78**, 4489-4497.

Long, C.E. and J.M. Oltman-Shay, 1991, "Directional characteristics of waves in shallow water," *Tech. Report CERC-91-1.*

Longuet-Higgins, M.S. and R.W. Stewart, 1962, "Radiation stresses and mass transport in gravity waves, with application to 'surf beat'," *J. Fluid Mech.*, **13**, 481-504.

Longuet-Higgins, M.S. and R.W. Stewart, 1964, "Radiation stress in water waves: A physical discussion, with applications," *Deep Sea Res.*, **11**, 529-562.

Munk, W.H., 1949, "Surf beats," *EOS Trans. AGU*, **30**(6), 849-854.

Okihiro, M., R.T. Guza, and R.J. Seymour, 1992 (accepted), "Bound Infragravity Waves," *J. Geophys. Res.*

Oltman-Shay, J.M. and R. T. Guza, 1987, "Infragravity edge wave observations on two California beaches," *J. Phys. Oceanogr.*, **17**, 644-663.

Oltman-Shay, J., P.A. Howd, and W.A. Birkemeier, 1989, "Shear Instabilities of the mean longshore current,

2: Field data," *J. Geophys. Res.*, 94, 18031-18043.

Oltman-Shay, J. and P.A. Howd, 1992 (accepted), "Edge Waves in Nonplanar Bathymetry and Moderate Alongshore Current: A Model and Field Comparison," *J. Geophys. Res.*

Oltman-Shay, J., P.A. Howd, R.A. Holman, R.T. Guza and E.B. Thornton, 1992 (submitted), "Evidence of high mode infragravity edge waves in the nearshore," *J. Geophys. Res.*

Pawka, S., 1982, "Wave directional characteristics on a partially sheltered coast," Ph.D. dissertation, 246 pp., Scripps Inst. of Oceangraphy, UCSD.

Pawka, S.S., 1983, "Island shadows in wave directional spectra," *J. Geophys. Res.*, **88**, 2579-2591.

Sand, Stig E., 1982, "Wave grouping described by bounded long waves," *Ocean Eng.*, 9(6), 567-580.

Sallenger, A.H. and R.A. Holman, 1984, "On predicting infragravity energy in the surf zone," *Proc. 19th Coastal Eng. Conf., ASCE*, 1940-1951.

Schaffer, H.A. and I.A. Svendson, 1988, "Surf beat generation on a mild-sloping beach," *Proc. of Coastal Eng. Conf.*, 1058-1072.

Schaffer, H.A., 1990, "Infragravity water waves induced by short-wave groups," Ph.D. dissertation, Series Paper #50, Institue of Hydrodynamics and Hydraulic Engineering, Technical University of Denmark. 168 pp.

Short, A.D., 1975, "Multiple offshore bars and standing waves," *J. Geophys. Res.*, **80**, 38383-3912.

Symonds, G., D.A. Huntley and A.J. Bowen, 1982, "Two-dimensional surf beat: longwave generation by a time-varying breakpoint," *J. Geophys. Res.*, **87**, 492-498.

Tucker, M.J., 1950, "Surf beats: Sea waves of 1 to 50 minute periods," *Proc. R. Soc. London, Ser. A*, 202, 565-573.

Table 1a. Linear regression analysis of infragravity, sea and swell wave variance

Variance Quantities	Sea		Swell	
	Correlation (C).	Regress. Slopes (R)	Correlation (C)	Regress. Slopes (R)
Infragravity	C=0.061	R=	C=0.095	R=
Trapped	C=0.060	R=	C=0.095	R=
Leaky	C=0.040	R=	C=0.062	R=
Edge Wave	C=0.062	R=	C=0.094	R=

Table 1b. Linear regression analysis of infragravity, sea and swell wave directional variance

Variance Quantities	NE Sea	SE Sea	NE Swell	SE Swell
Northward Edge Waves	C=0.076 R=	C=0.040 R=	C=0.096 R=	C=0.054 R=
Southward Edge Waves	C=0.050 R=	C=0.076 R=	C=0.038 R=	C=0.095 R=

Figure Captions

Figure 1. Perspective view of the SAMSON and DELILAH field site and instrument locations. Shown are the locations of the pier (vertical pole connected to shore), surf zone current and pressure sensor arrays (vertical poles), 8 m depth array and 13 m depth pressure sensor arrays (black dots). Note the scour hole under the pier and the alongshore-aligned sand bar close to shore. NGVD is 10 cm above mean sea level (MSL).

Figure 2. October 1990: Observed significant wave heights of surface gravity waves in the infragravity (0.005-0.05 Hz), swell (0.05-0.15 Hz) and sea (0.15-0.30 Hz) frequency bands. Wave heights are obtained by surface correcting (with linear theory) bottom pressure measurements from one sensor in 8m depth.

Figure 3. IMLE estimated alongshore cyclic wavenumber (reciprocal wavelength)-frequency spectrum from the 800 m offshore linear array of bottom pressure. The rectangular boxes mark the location of variance peaks, defined as those wavenumber maxima having an adjacent valley below their half-power. Their wavenumber width defines their half-power bandwidth. Shading indicates log variance density within the half-power bandwidth. The solid lines marked d.w. disp and local disp are the deep water and local depth dispersion curves. Also drawn is the mode 0 edge wave dispersion curve for this beach. $\Delta f = 0.00195$ Hz, d.o.f. = 38.

Figure 4. Integration boundaries for partitioning of trapped, leaky and edge wave variance.

Figure 5. Ratio of edge wave to total infragravity wave variance observed over 8 months. Days are numbered from September 1, 1990 (Julian number = 24X) to April 31, 1991 (Julian number = 355+xxx).

Figure 6. Scatter plots of infragravity variance against sea and swell wave variance

Figure 7. Scatter plots of edge wave directional variance against sea and swell directional variance.

Figure 8. Scatter plots of edge wave directional variance against swell directional variance.

Figure 9. Wave triad difference interaction diagrams for the resonant excitation of different edge wave modes; a) swell-swell wave interactions, b) sea-sea wave interactions).

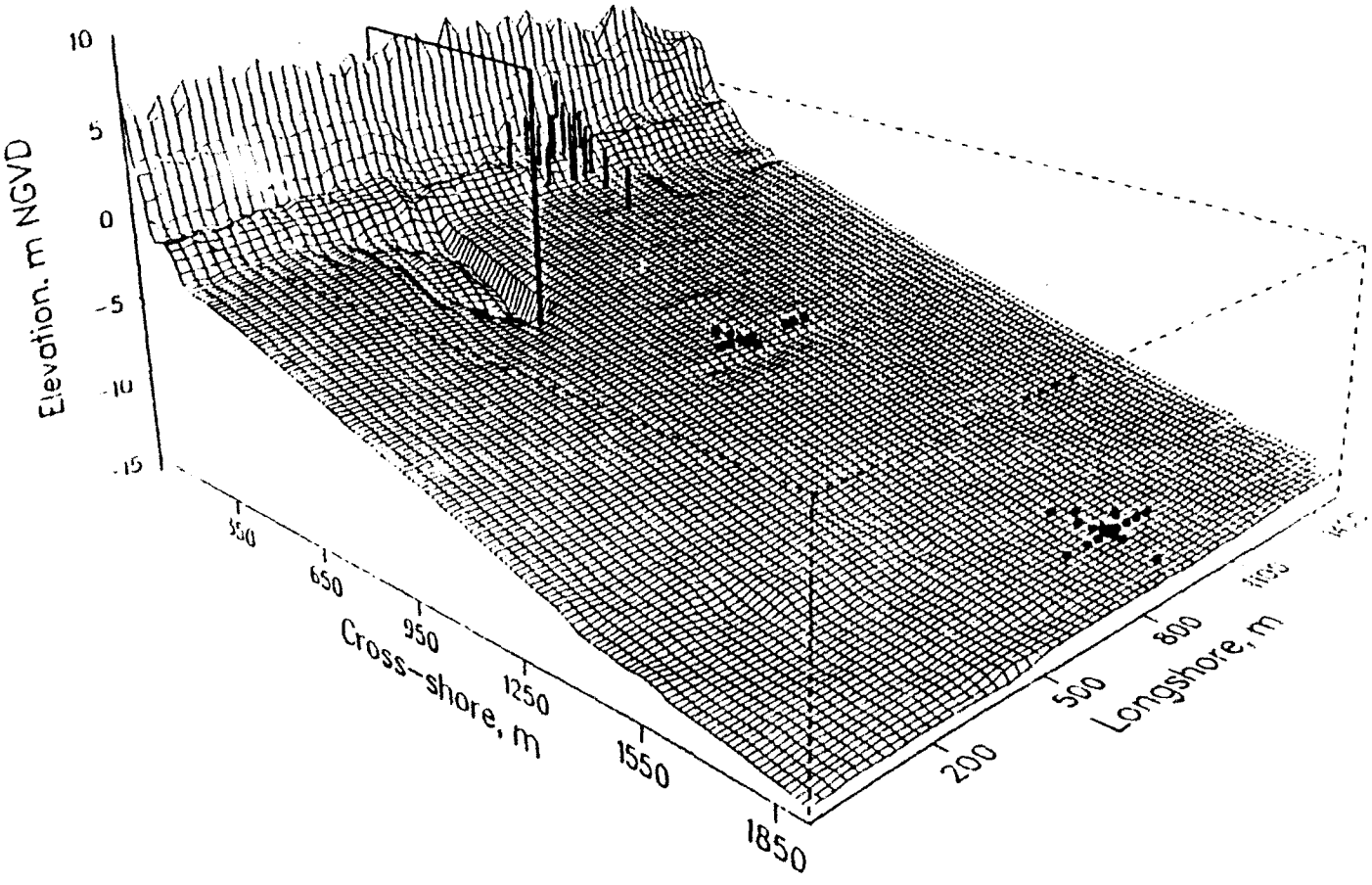
Elevation, m NGVD
10
5
0
-5
-10
-15
350
650
950
1250
1550
1850
Cross-shore, m
200
500
800
Longshore, m

Fig. 1

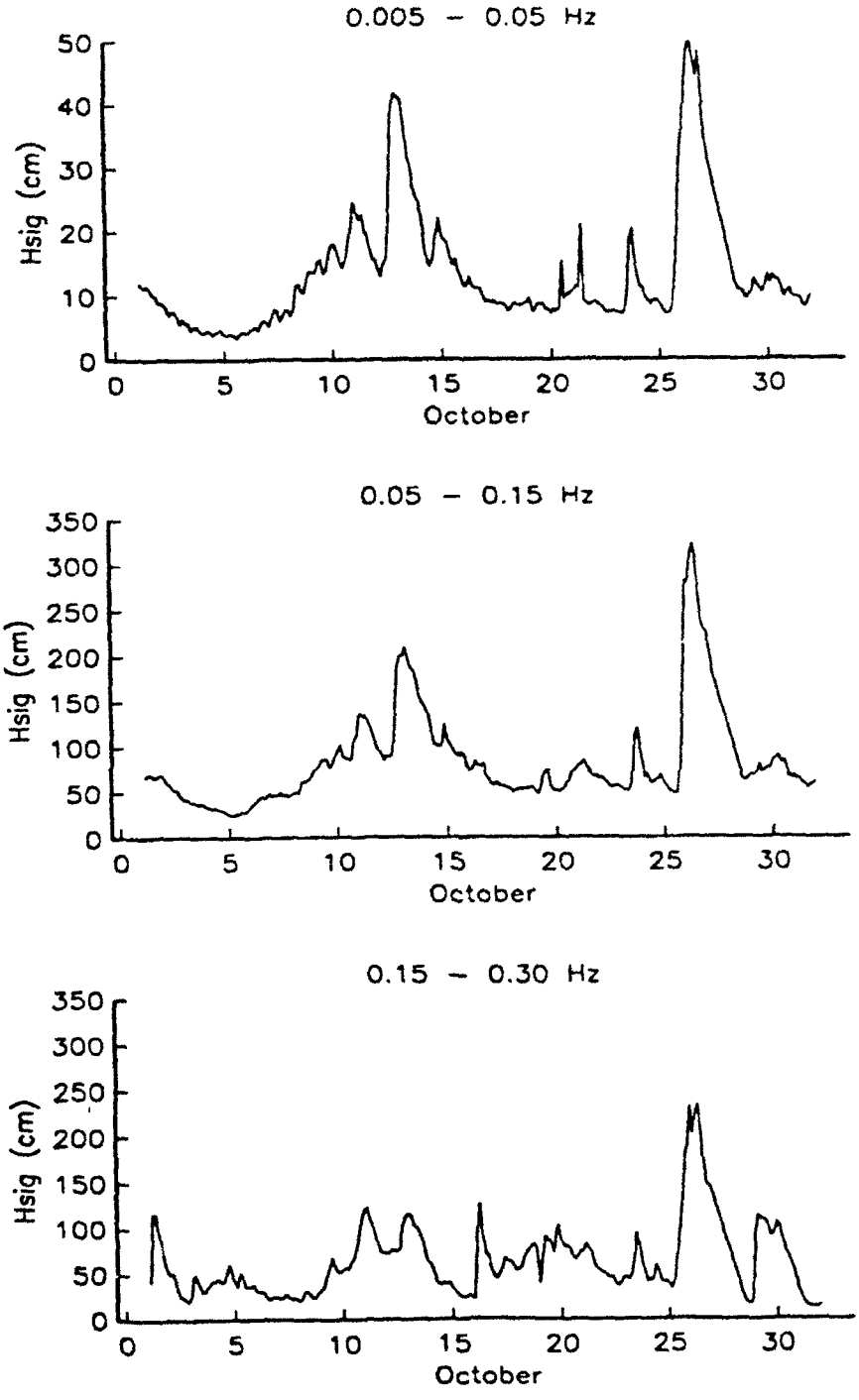
0.005 – 0.05 Hz
Hsig (cm)
50
40
30
20
10
0
0
5
10
15
20
25
30
October
0.05 – 0.15 Hz
Hsig (cm)
350
300
250
200
150
100
50
0
0
5
10
15
20
25
30
October
0.15 – 0.30 Hz
Hsig (cm)
350
300
250
200
150
100
50
0
0
5
10
15
20
25
30
October

Figure 2

a.

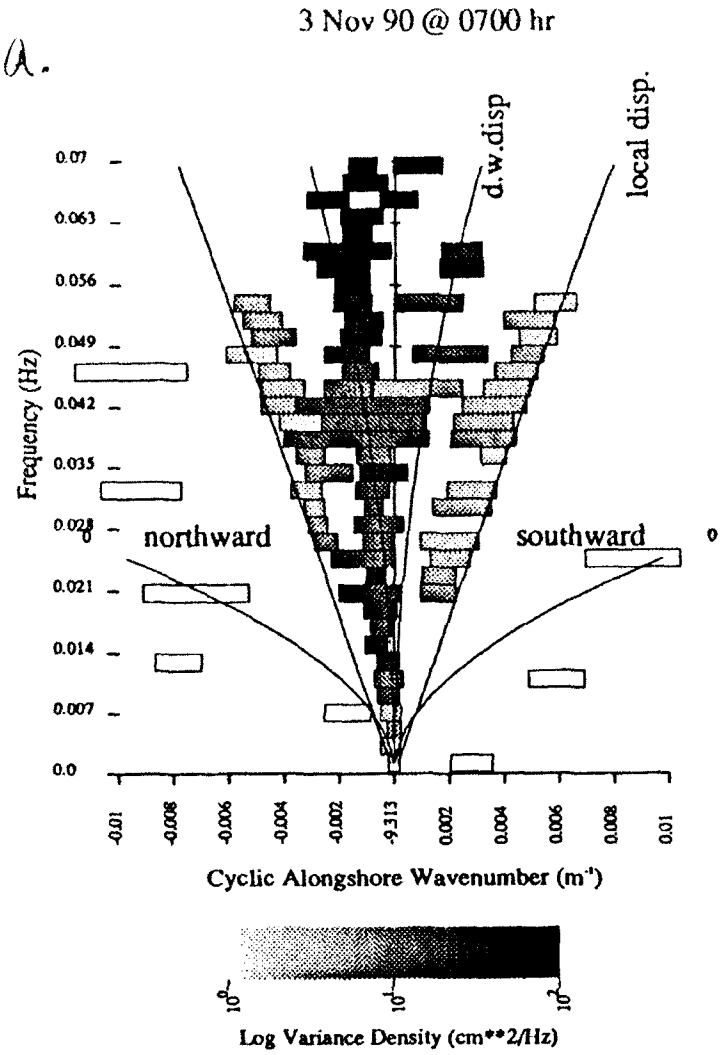
3 Nov 90 @ 0700 hr
d.w.disp
local disp.
Frequency (Hz)
0.07
0.063
0.056
0.049
0.042
0.035
0.028
0.021
0.014
0.007
0.0
northward
southward
0
-0.01
-0.008
-0.006
-0.004
-0.002
-9.313
0.002
0.004
0.006
0.008
0.01
Cyclic Alongshore Wavenumber (m⁻¹)
10⁰
10⁻¹
10⁻²
Log Variance Density (cm**2/Hz)

b.

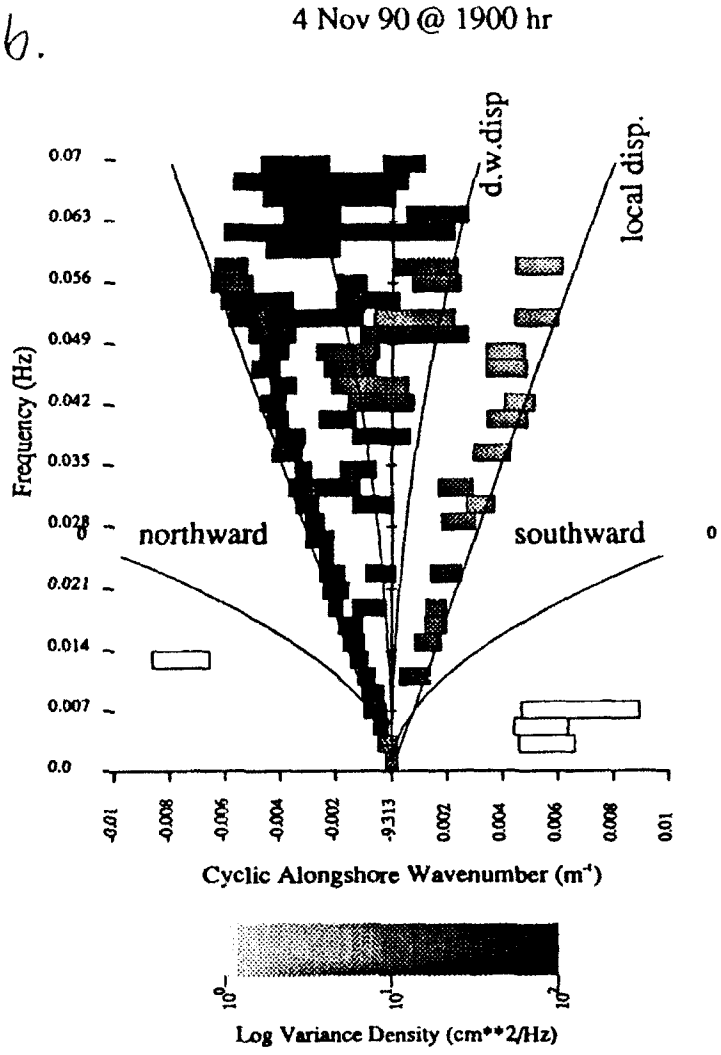
4 Nov 90 @ 1900 hr
d.w.disp
local disp.
Frequency (Hz)
0.07
0.063
0.056
0.049
0.042
0.035
0.028
0.021
0.014
0.007
0.0
northward
southward
0
-0.01
-0.008
-0.006
-0.004
-0.002
-9.313
0.002
0.004
0.006
0.008
0.01
Cyclic Alongshore Wavenumber (m⁻¹)
10⁰
10⁻¹
10⁻²
Log Variance Density (cm**2/Hz)

Fig 3

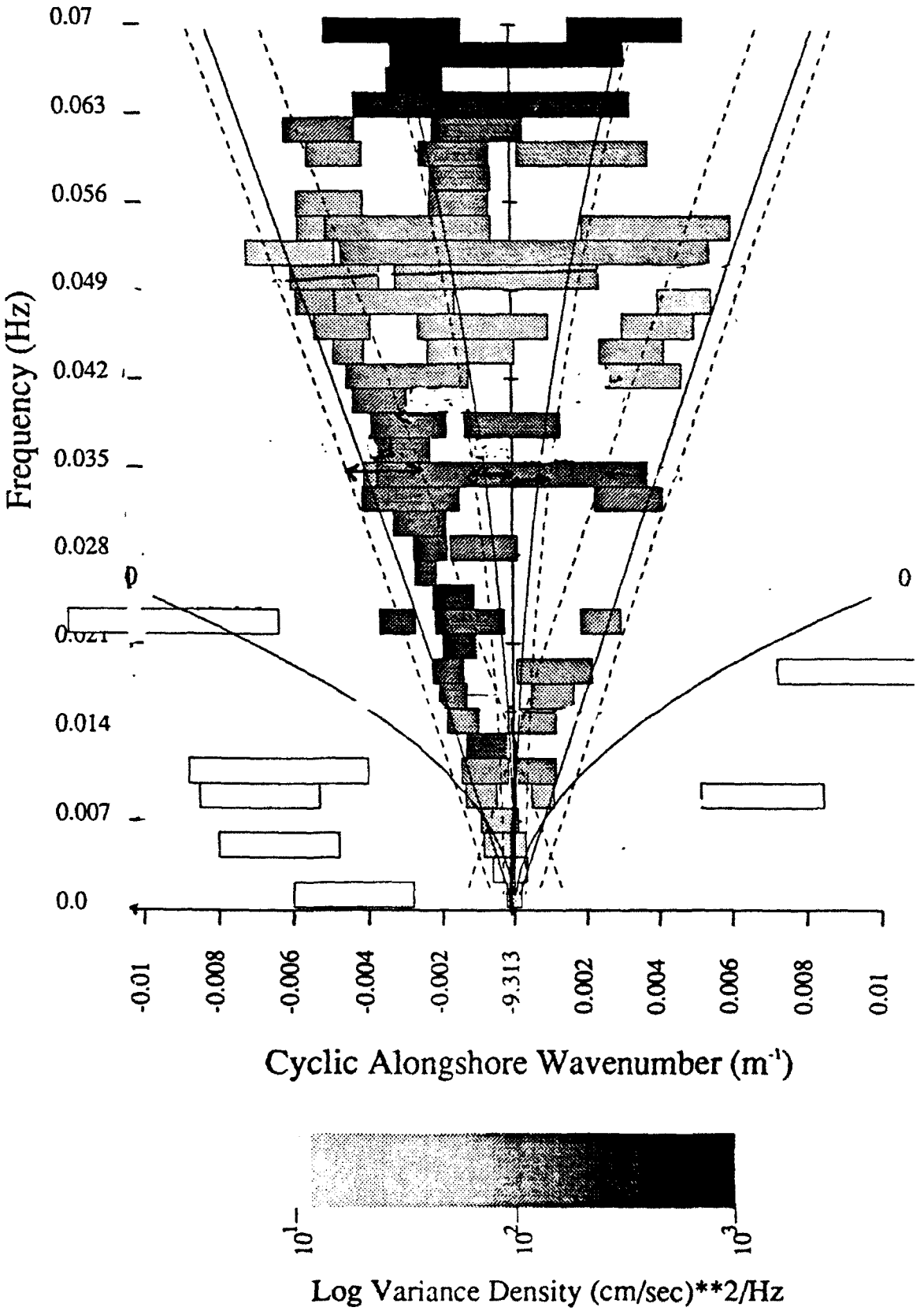
0.07
0.063
0.056
0.049
0.042
0.035
0.028
0.021
0.014
0.007
0.0
Frequency (Hz)
0
0
-0.01
-0.008
-0.006
-0.004
-0.002
-9.313
0.002
0.004
0.006
0.008
0.01
Cyclic Alongshore Wavenumber (m-1)
10-1
102
103
Log Variance Density (cm/sec)**2/Hz

Fig 4

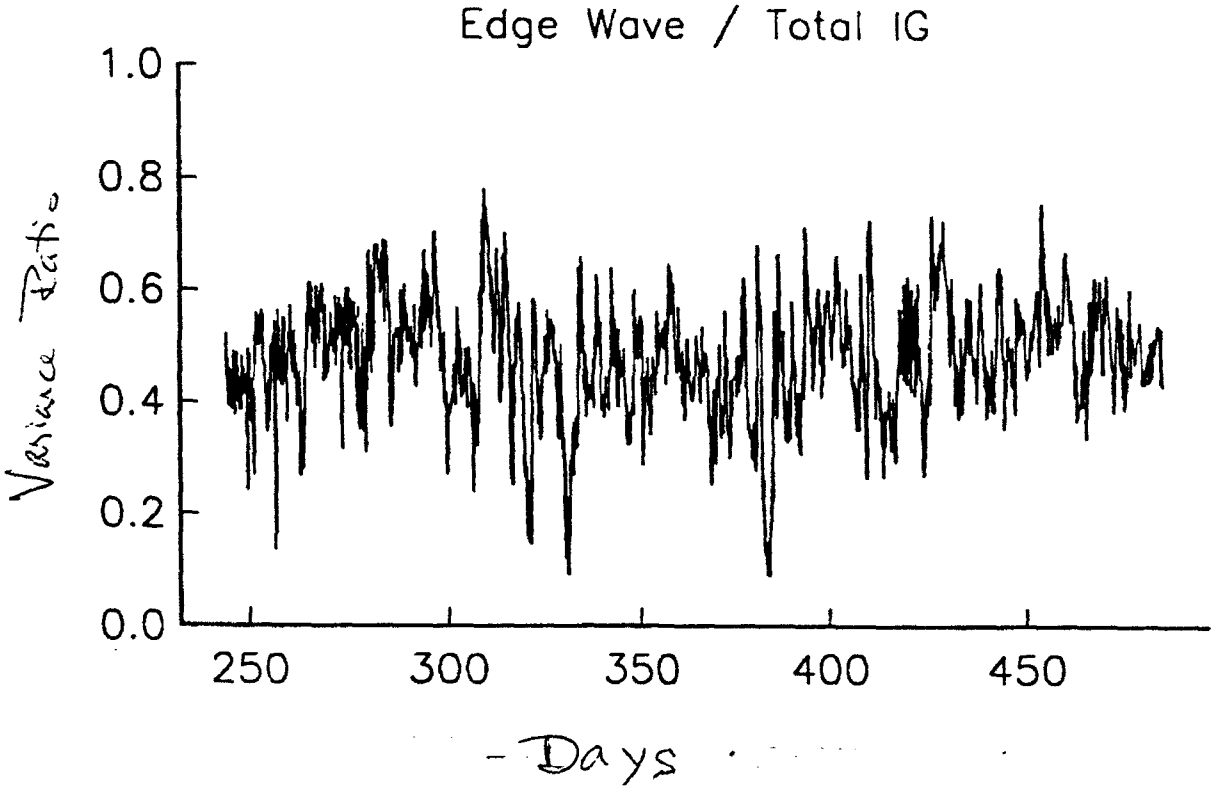
Edge Wave / Total IG
1.0
0.8
0.6
0.4
0.2
0.0
Variance Ratio
250
300
350
400
450
- Days

Fig 5

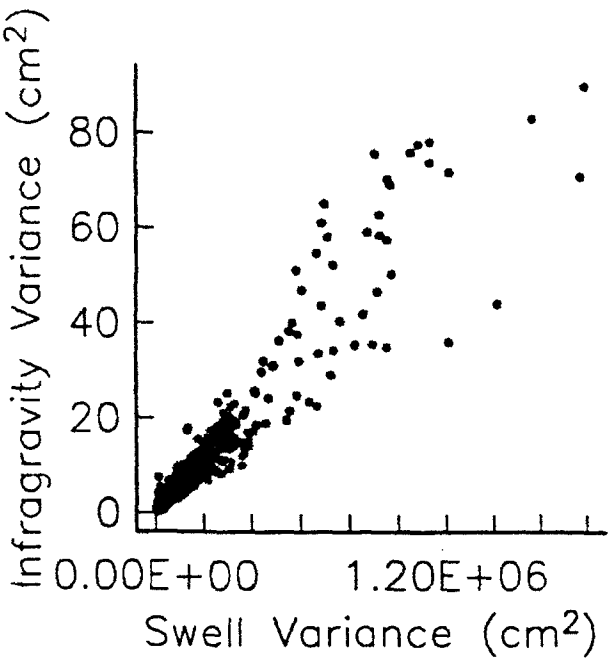
Infragravity Variance (cm²)
0
20
40
60
80
0.00E+00
1.20E+06
Swell Variance (cm²)

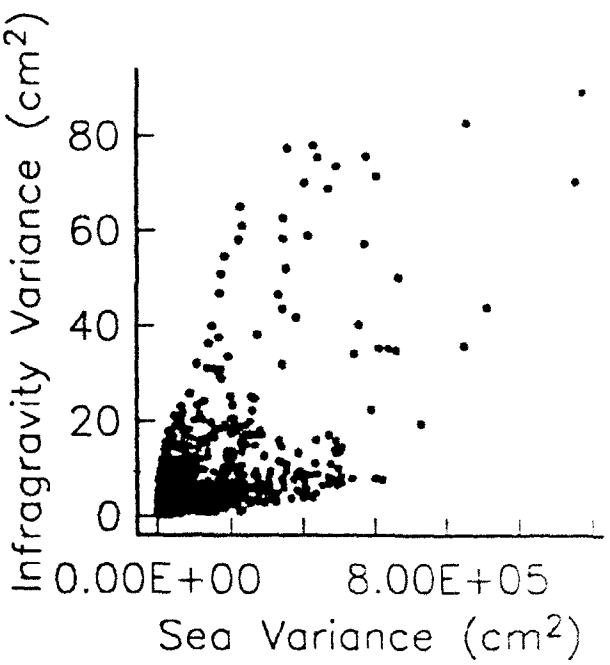
Infragravity Variance (cm²)
0
20
40
60
80
0.00E+00
8.00E+05
Sea Variance (cm²)

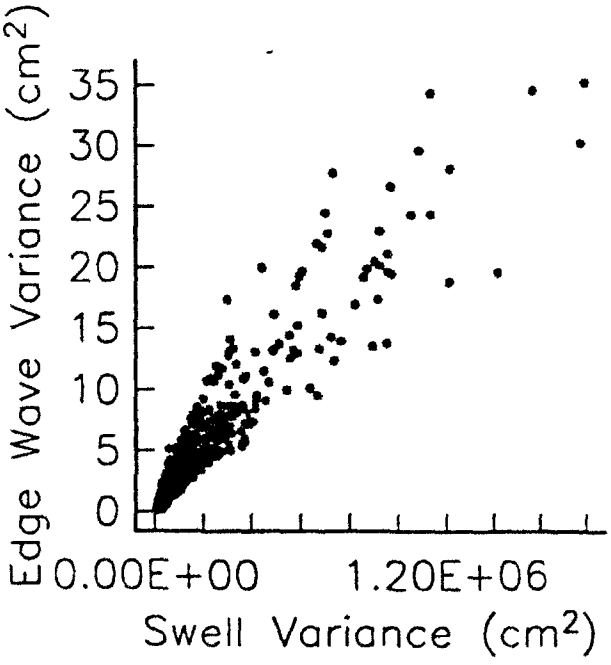
Edge Wave Variance (cm²)
0
5
10
15
20
25
30
35
0.00E+00
1.20E+06
Swell Variance (cm²)

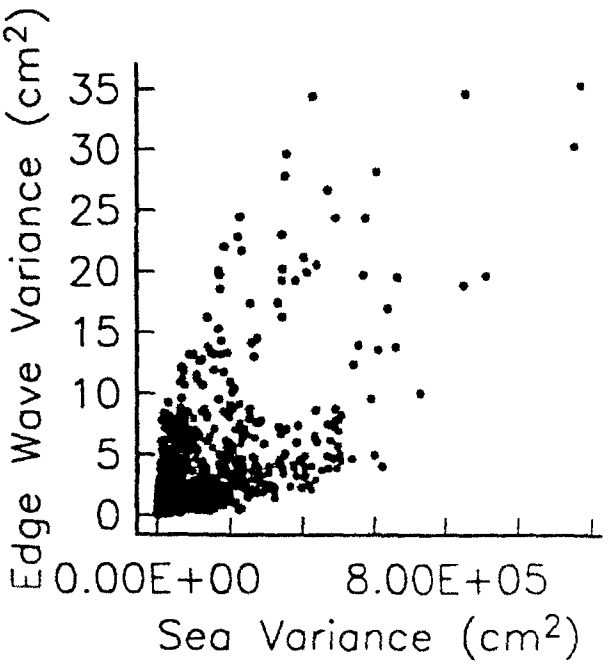
Edge Wave Variance (cm²)
0
5
10
15
20
25
30
35
0.00E+00
8.00E+05
Sea Variance (cm²)

Fig 6

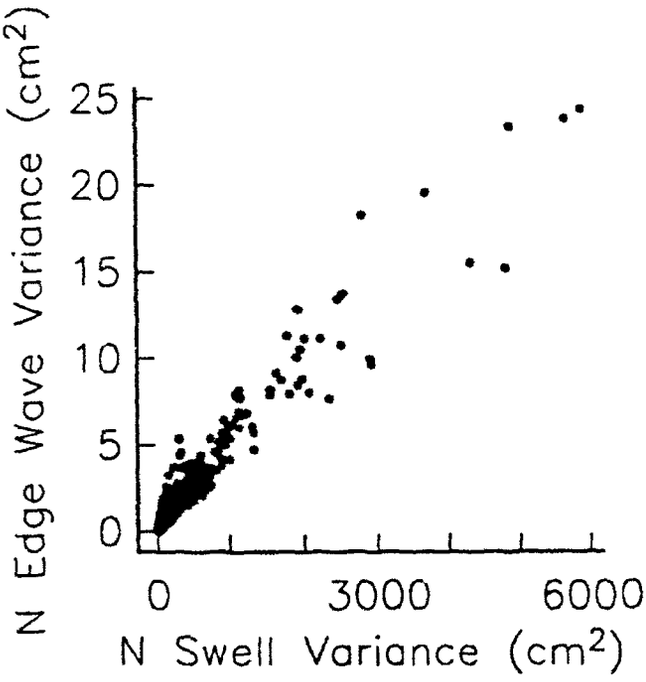
N Edge Wave Variance (cm²)
25
20
15
10
5
0
0
3000
6000
N Swell Variance (cm²)

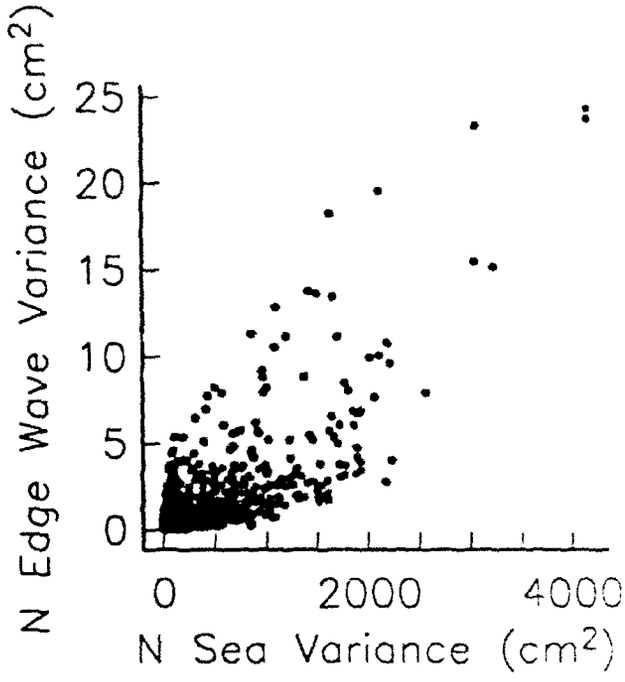
N Edge Wave Variance (cm²)
25
20
15
10
5
0
0
2000
4000
N Sea Variance (cm²)

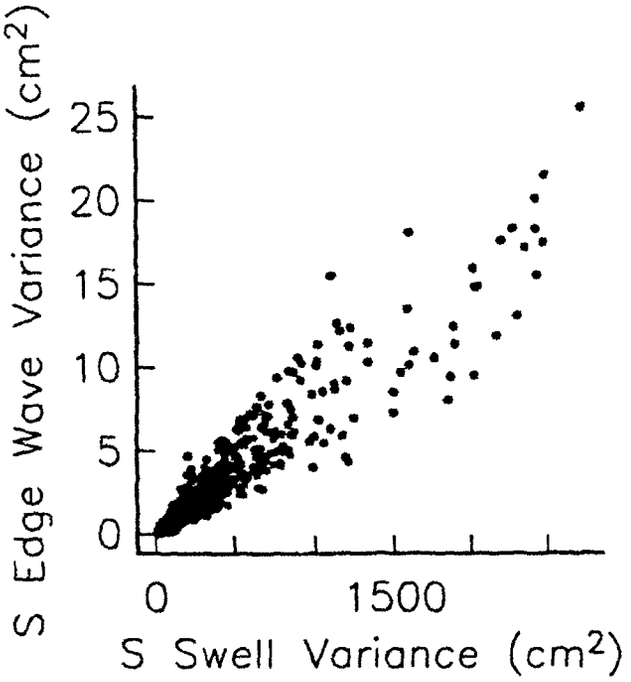
S Edge Wave Variance (cm²)
25
20
15
10
5
0
0
1500
S Swell Variance (cm²)

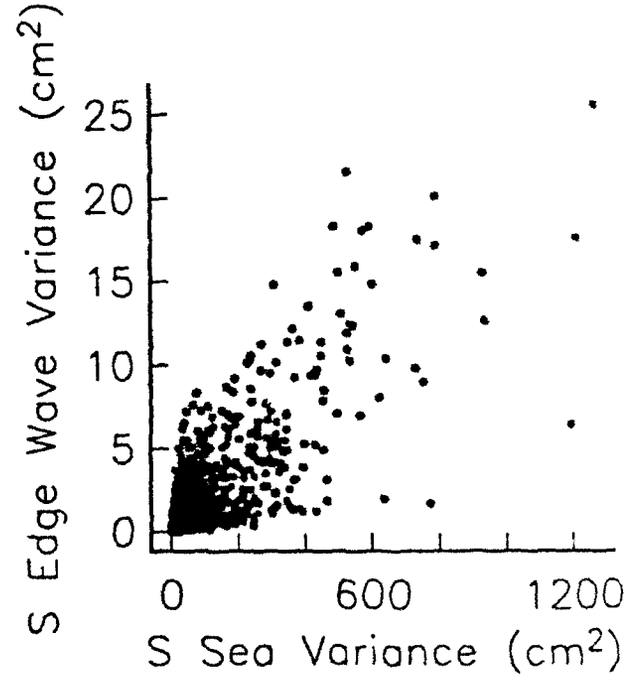
S Edge Wave Variance (cm²)
25
20
15
10
5
0
0
600
1200
S Sea Variance (cm²)

Fig 7

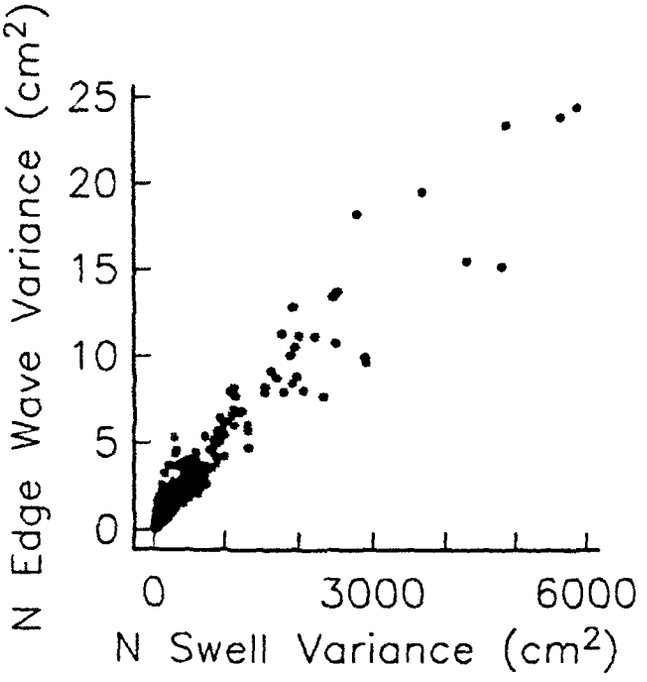
N Edge Wave Variance (cm²)
25
20
15
10
5
0
0
3000
6000
N Swell Variance (cm²)

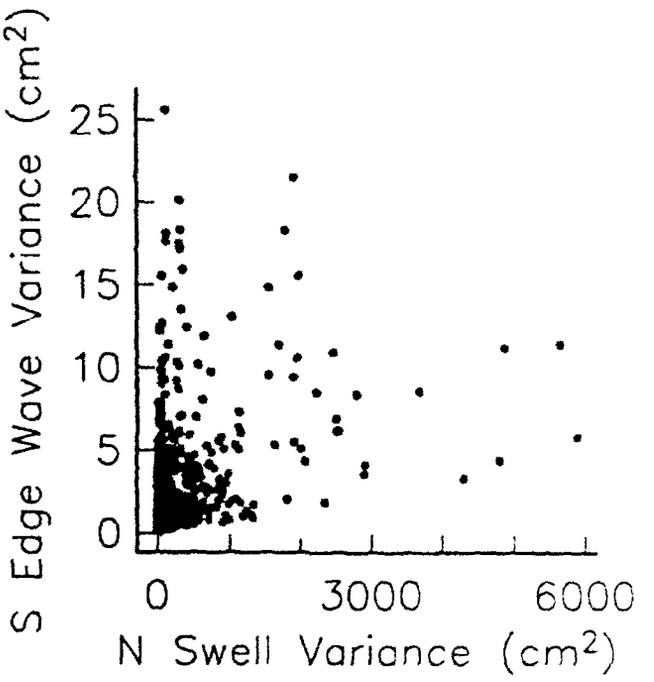
S Edge Wave Variance (cm²)
25
20
15
10
5
0
0
3000
6000
N Swell Variance (cm²)

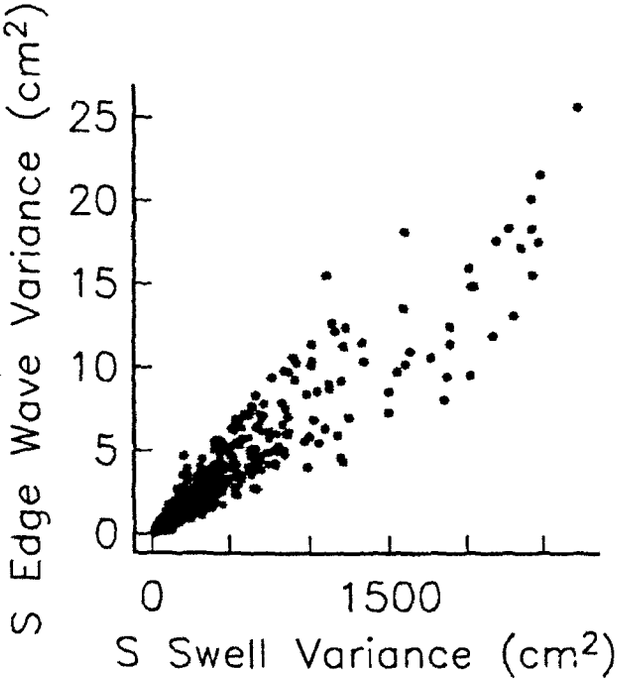
S Edge Wave Variance (cm²)
25
20
15
10
5
0
0
1500
S Swell Variance (cm²)

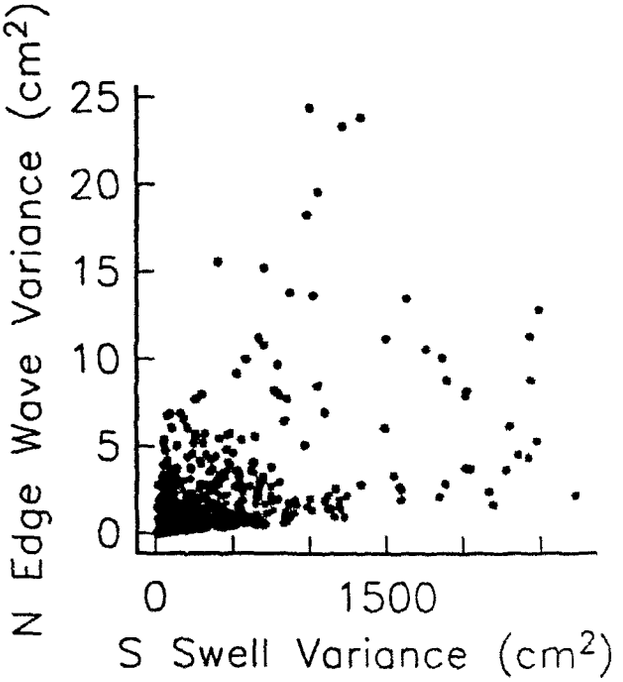
N Edge Wave Variance (cm²)
25
20
15
10
5
0
0
1500
S Swell Variance (cm²)

Fig 8

a. SWELL-SWELL INTERACTIONS

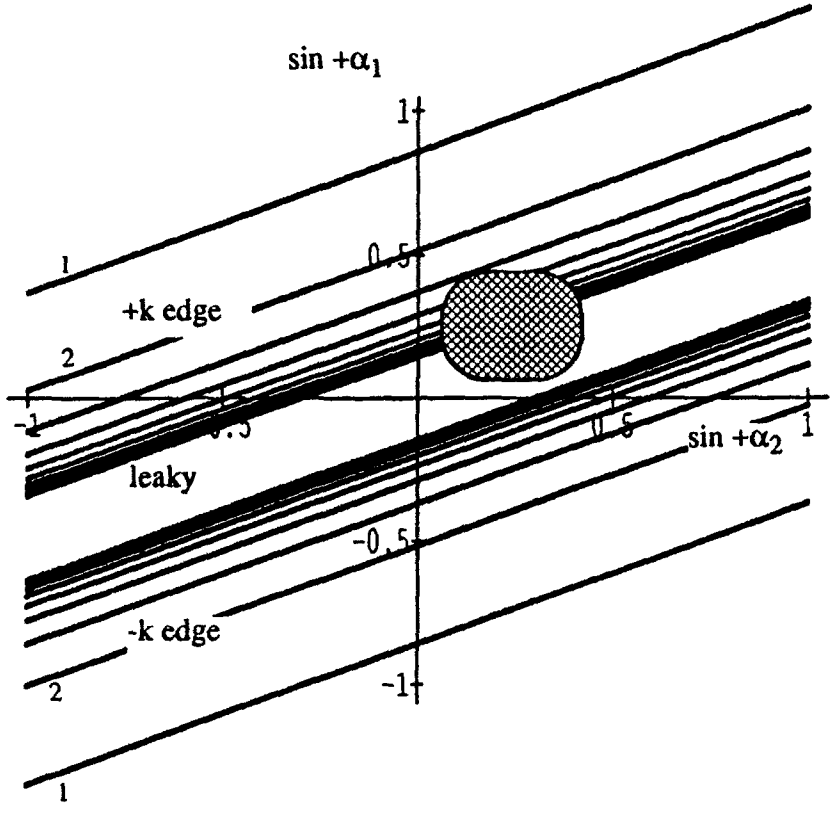

b. SEA-SEA INTERACTIONS

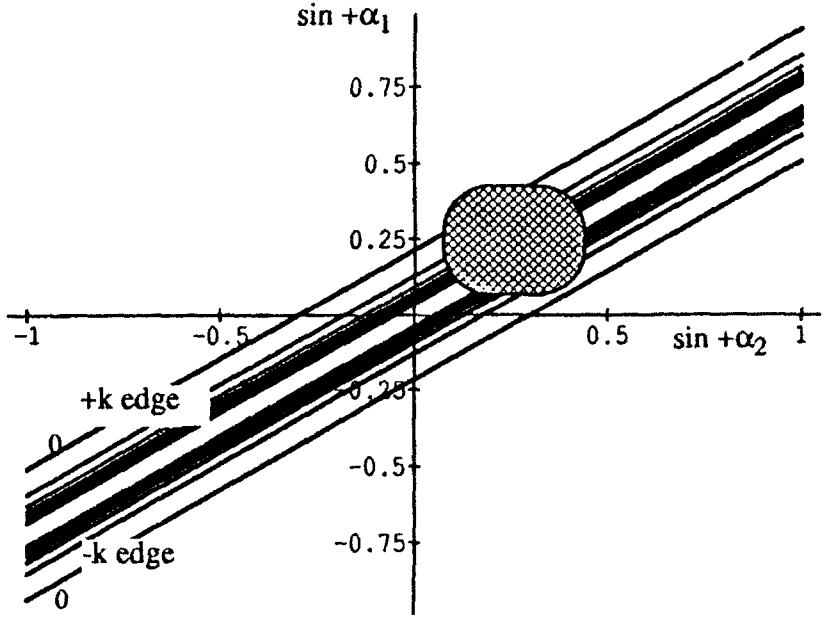

Fig 7